Multi-Section Waveguide Method for Facet Temperature Reduction and Improved Reliability of High-Power Laser Diodes

Kaveh Ebadi[1], Yuxian Liu[2,3], Ali Kaan Sünnetçioğlu[1], Sinan Gündoğdu[1], Serdar Şengül[1], Yuliang Zhao[2,3], Yu Lan[2,3], Guowen Yang[2,3,4], Abdullah Demir[1,*]

[1]Bilkent University, UNAM - Institute of Materials Science and Nanotechnology, Ankara, Turkey, 06800

[2]State Key Laboratory of Transient Optics and Photonics, Xi'an Institute of Optics and Precision Mechanics, Chinese Academy of Sciences, Xi'an, China, 710119

[3]University of Chinese Academy of Sciences, Beijing, China, 100049

[4]Dogain Laser Technology (Suzhou) Co., Ltd., Suzhou, China, 215123

ABSTRACT

Catastrophic optical mirror damage (COMD) limits the output power and reliability of lasers diodes (LDs). Laser self-heating together with facet absorption of output power cause the facet to reach a critical temperature (T_c), resulting in COMD and irreversible device failure. The self-heating of the laser contributes significantly to the facet temperature, but it has not been addressed so far. We implement a multi-section waveguide method where the heat is separated from reaching the output facet by exploiting an electrically isolated window. The laser waveguide is divided into two electrically isolated laser and transparent window sections. The laser section is pumped at high current levels to achieve laser output, and the passive waveguide is biased at low injection currents to obtain a transparent waveguide with negligible heat generation. Using this design, we demonstrate facet temperatures lower than the junction temperature of the laser even at high output power operation. While standard LDs show COMD failures, the multi-section waveguide LDs are COMD-free. Our technique and results provide a pathway for high-reliability LDs, which would find diverse applications in semiconductor lasers.

1. INTRODUCTION

GaAs-based high-power LDs have evolved drastically to be used in industrial applications [1,[2]]. Although they have the highest electro-optical conversion efficiency and record output power levels [3,4,5], the primary problem limiting the reliable output power of LDs is still COMD at the output facet, which has been studied extensively [6, 7]. COMD limits the performance of the LDs and directly affects fiber and solid-state lasers that rely on high-power LDs as pump sources. Therefore, a method for solving COMD in LDs directly improves the performance, reliability and cost of modern high-power fiber, direct-diode and solid-state lasers.

In general, heat adversely affects the electronic and optoelectronic device performance and lifetime. In LDs, self-heating contributes the most to laser facet heating, causing the facet to reach a critical temperature (T_c), resulting in a feedback mechanism resulting in COMD and device failure [7]. Many attempts have been reported in the literature to address this issue, such as the current blocking layer near the output facet [8], non-absorbing mirror (NAM) [9], ultra-high vacuum (UHV) passivation [10], passivation of air-exposed surface states [11] and quantum well intermixing [12, 13, 14].

[*]abdulllah.demir@unam.bilkent.edu.tr

Semiconductor Lasers and Laser Dynamics X, edited by Marc Sciamanna,
Krassimir Panajotov, Sven Höfling, Proc. of SPIE Vol. 12141, 1214104
© 2022 SPIE · 0277-786X · doi: 10.1117/12.2621651

Implementing such approaches can mitigate the facet's heat generation mechanisms (e.g., optical absorption, non-radiative recombination). Thus, reducing facet temperatures and consequently improving COMD level [15, 16]. These approaches focus mainly on the heating caused by the facet itself; however, the self-heating of the laser contributes significantly to the facet temperature, which has not been addressed so far.

This study uses a multi-section waveguide method shown in Figure 1 to effectively isolate laser heat load from the output facet, which dramatically reduces facet temperature even below the laser cavity temperature developed in our previous work [17, 18]. We fabricated and carried out detailed characterization of the devices, studied their optimum working conditions (i.e., identical output power with much lower facet temperature than the standard LDs), and revealed elimination of COMD in LDs. The LDs waveguide is divided into two sections, laser and passive waveguide, which gives electrical and thermal isolation. The laser section is responsible for the lasing action pumped at high current levels (I_{las}), and the waveguide section is biased at low injection current (I_{win}), to acquire a transparent waveguide with minor heat generation. Exploiting this design restricts the thermal load from the laser section reaching the facet.

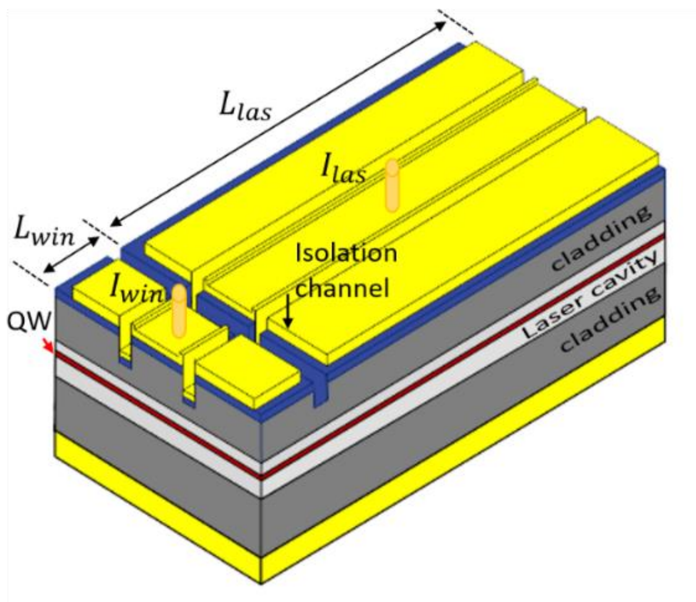

Figure 1. The schematic of the multi-section LD.

2. FACET TEMPERATURE MEASUREMENT SETUP

In this paper, we employed a high-efficiency GaAs-based epitaxial structure with a single quantum well (QW) active region [19, 20]. Fabricated GaAs-based 915 nm LDs have 100 µm waveguides with a total cavity length (laser and window sections) of 5.0 mm. Five designs with L_{win}=0, 250, 500,1000,1500 µm are fabricated to study the multi-section LDs systematically. In this study we utilized CMOS based-thermoreflectance (TR) method (Figure 2) to obtain facet temperatures of LDs. it is a well-established surface temperature measurement method have been used in many applications [21, 22, 23]. Its principle is based on the dependence of the relative change in reflectivity due to temperature change and given as:

$$\frac{\Delta R}{R} = \left(\frac{1}{R}\frac{\partial R}{\partial T}\right)\Delta T = \kappa\Delta T \qquad (1)$$

where ΔR/R is a relative change in reflectivity, ΔT is a temperature change, R is the reflection coefficient, and κ is the TR coefficient, which depends on the material properties together with optical parameters of the TR setup such as illumination wavelength, and NA of the objective [24]. A LED at λ= 470 nm is used as the probe signal focused on the laser facet through a (50X, 0.6 NA) PAL-50-NIR-HR-LC00 objective after passing through a condenser lens, beam splitter (BS), and a dichroic mirror (DM) transmitting LED light while reflecting 99% of the laser beam. An OD 6 filter with a band-pass around LED wavelength is used to block laser emission from reaching the camera while transmitting probe signal having facet temperature information. Exploiting our setup, we achieved ≈ 0.5 K temperature and ≈ 0.5 μm spatial resolution. The reflected beam from the DM is coupled into an integrating sphere to read LD power and wavelength, which are used to measure the junction temperature of the LD. The measurements, LDs are driven by square wave currents at the frequency 5 Hz (i.e., pulse width=100 ms and duty cycle=50 %) while camera is triggered by a square wave having 10 Hz frequency to collect an image at each time interval that laser is on and off. I_{win} in multi-section lasers is driven using a continuous wave (CW) current source.

Utilizing equation (1), we calculate the TR coefficient (κ) by recording TR signal (ΔR/R) for a known ΔT by varying the heatsink temperature with small steps over an extensive temperature range resulting in κ of the setup as $(1.8\pm0.1)\times10^{-4}$ K^{-1}. The laser is place on a carrier that is mounted on a TEC on top of a copper heatsink, and a fan is cooling down the heatsink.

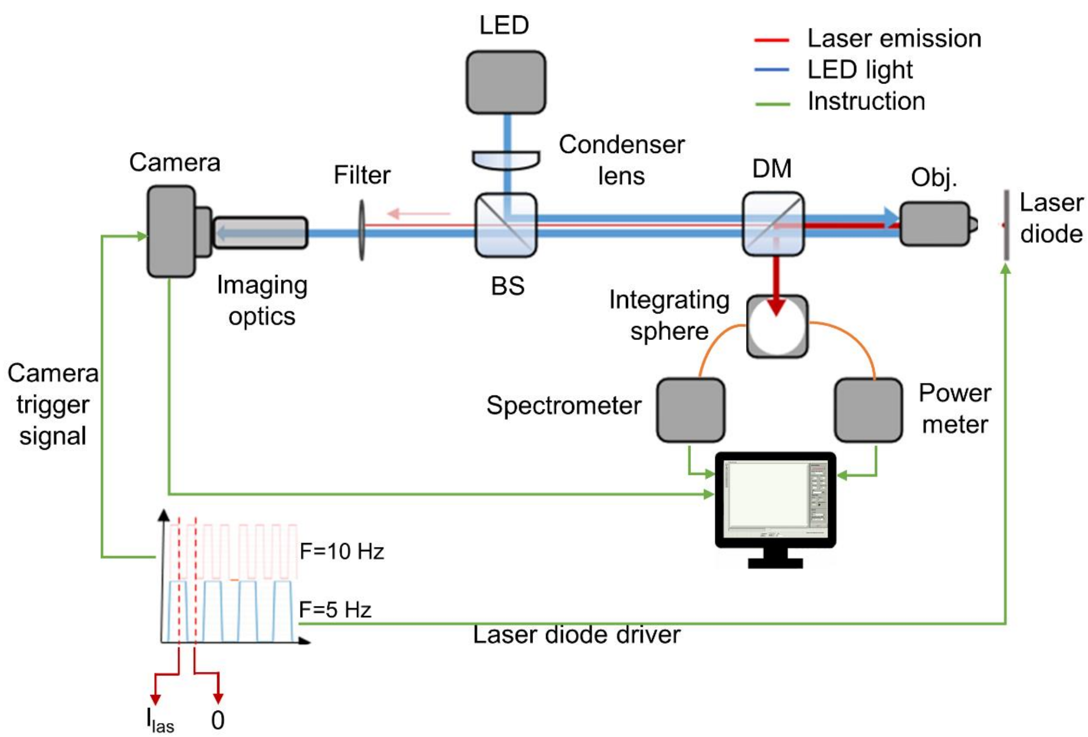

Figure 2. The schematic of the thermoreflectance setup.

3. RESULTS

We tested five different LD designs with L_{win}=0, 250, 500, 1000, 1500 μm to investigate their temperature and electro-optical characteristics. First, we started characterizing LDs with I_{win}=0 and then analyzed how I_{win} affects their behavior.

Eventually, we focused on multi-section LDs with L_{win} of 500 and 1000 µm, demonstrating the best performance compared to the standard LD (L_{win} =0 µm). Figure 3 illustrates the temperature characterization results of the multi-section and standard LDs with I_{win}=0 at I_{las}=8 A. Figure 3(a) depicts the design of the multi-section LD, and the enlarged image corresponds to the waveguide temperature map of the laser with L_{win}=1000 µm having the lowest temperature map. Figure 3.(b) displays the facet temperature maps of all the designs. The laser facet gets cooler with longer L_{win} due to thermally separating the laser heat-load from the output facet. Figure 3(c) shows the vertical temperature scans of (b) from the top of the epitaxial region to GaAs substrate where the solid lines show facet temperature, and the dashed lines show T_{las} at I_{las} =10 A for each chip. The facet and peak temperature for all multi-section LDs are lower than the standard LD. Additionally, even the peak T_{fac} is lower than T_{las} of any designs for L_{win} of 1000 and 1500 µm as shown in Figure 3.(d). Comparing these two designs indicates that the $T_{fac,peak}$ values are similar, implying that L_{win} of 1000 µm is long enough to isolate the laser heat load from the output facet. Therefore, we choose L_{win}=1000 µm LD for further analysis together with L_{win}=500 µm for comparison and standard laser (i.e., L_{win}=0) as a reference.

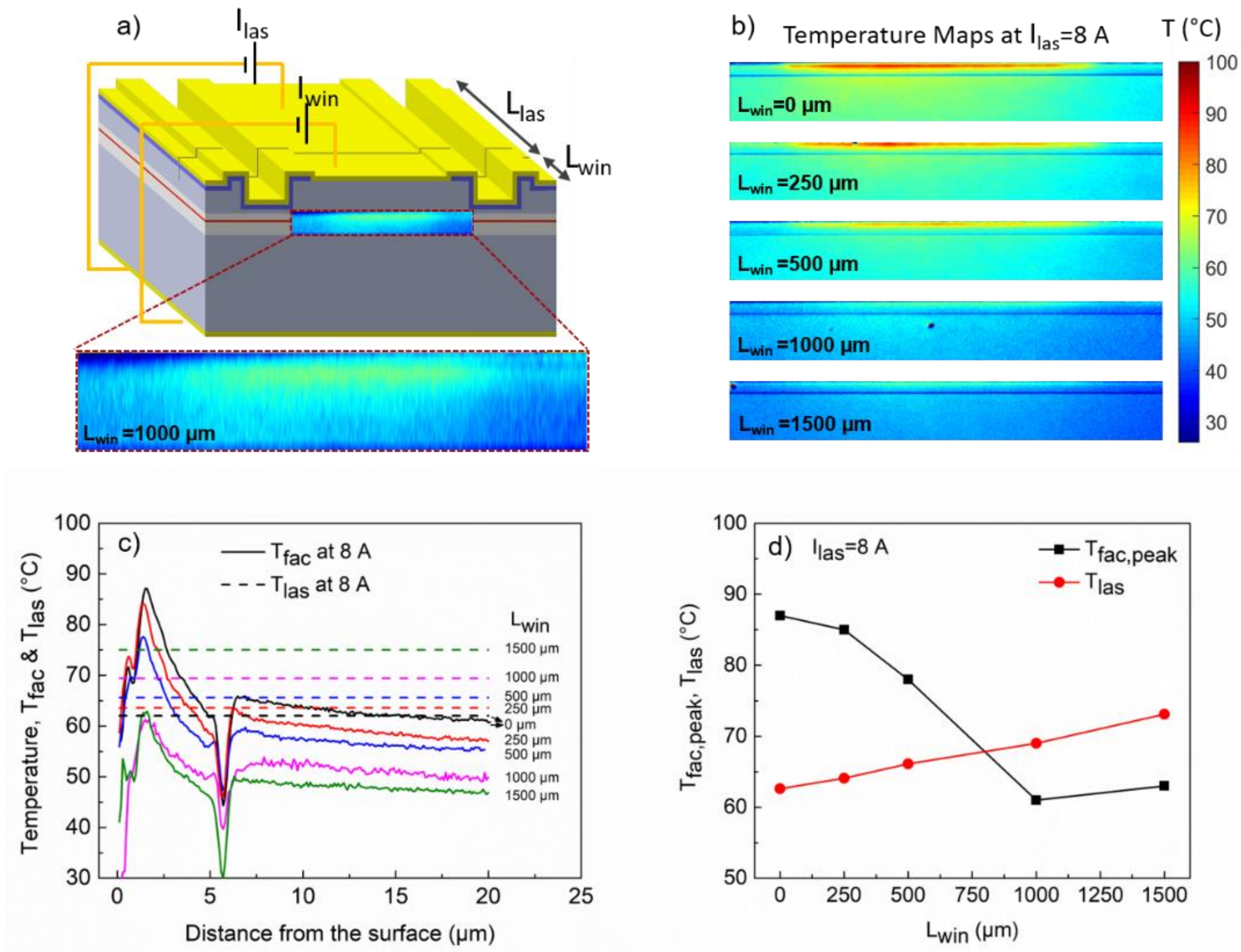

Figure 3. Temperature characteristics comparison of all LDs at I_{las} =8 A and I_{win}=0. (a) LD structure, enlarged image corresponds to the coolest facet for L_{win}=1000 µm. (b) Temperature distribution map for all LDs. (c) T_{fac} vs. distance from the top edge and T_{las} for I_{las} =8 A. (d) $T_{fac,peak}$ and T_{las} for each LD at I_{las} =8 A.

Figure 4 shows a comprehensive comparison of all the LDs investigated in this work where peak facet temperature, $T_{fac,\ peak}$ is plotted as a function of I_{las} where I_{win}= 0 A. At all current levels, the standards laser (L_{win}=0) has the highest $T_{fac,\ peak}$ followed by lasers having transparency window in front where the LD with L_{win}=1000 μm has the lowest $T_{fac,\ peak}$.

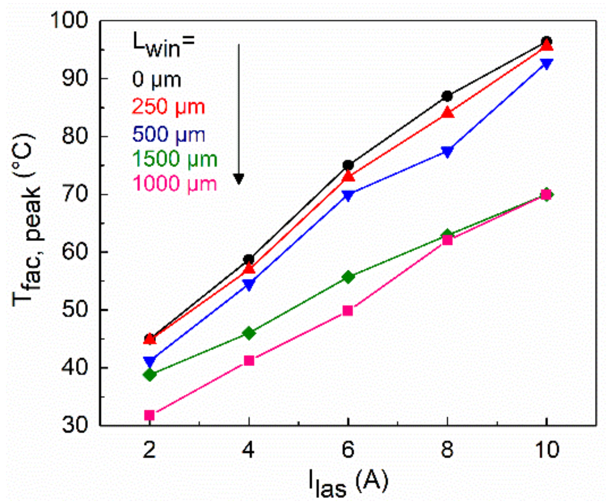

Figure 4. Peak facet temperature, $T_{fac,peak}$, vs. I_{las} comparison of all LDs studied in this work.

We know that I_{win}=0 leads to optical absorption losses in the unpumped window section. In addition to the power degradation of such a structure, the optical absorption of the laser output in the window section induces heat. Consequently, the window section must be electrically pumped to recover power losses and possibly eliminate the heat caused by the optical absorption. The measured CW L-I data for all LDs in Figure 5(a) indicate that the output power reduces as L_{win} increases. When L_{win} increases, I_{th} increases (not shown), indicating that the loss arises in the window section, which is more significant for the longer L_{win} than the shorter one. One can conclude this as a drawback for this structure. However, it is not; pumping I_{win} eliminates the absorption in this region, as mentioned before, and recovers the output power, as shown in Figure 5(b). Comparing the output power levels for L_{win} =500 μm (I_{win} =400 mA) and 1000 μm (I_{win}=800 mA) with the standard laser, the output power is similar for L_{win} =500 μm and even slightly higher for L_{win} =1000 μm.

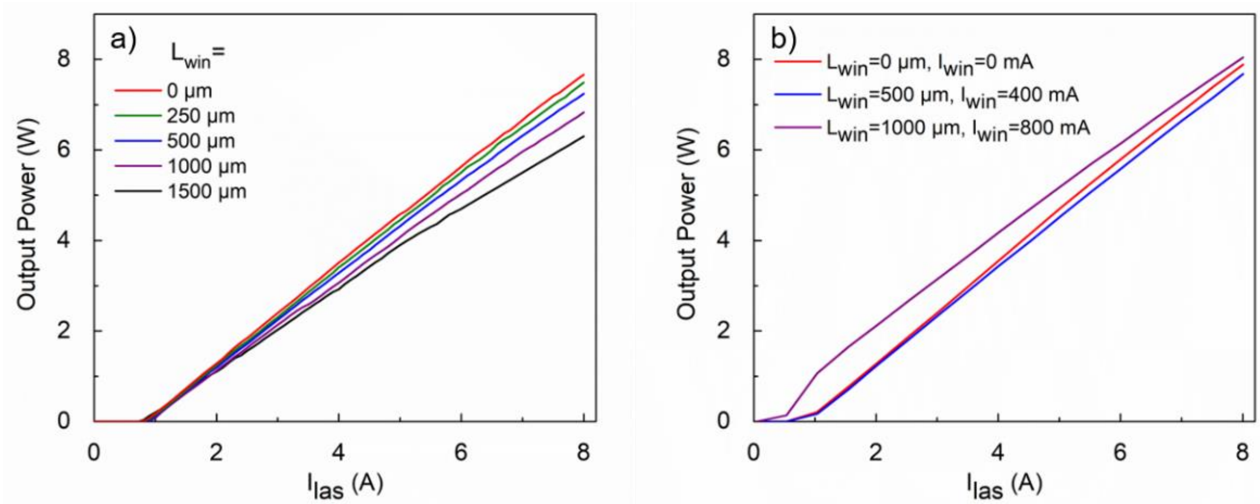

Figure 5. (a) Output power for all LDs as a function of I_{las}. (b) Output power for L_{win}=500 μm with I_{win}=400 mA, L_{win}=1000 μm with I_{win}=800 mA, and standard LD (L_{win}=0 μm).

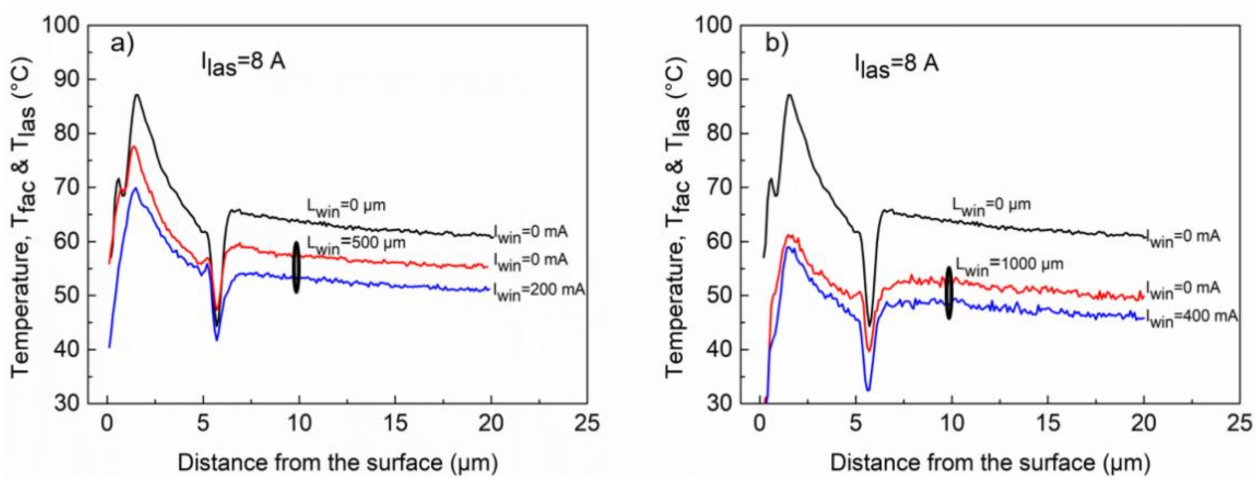

Figure 6 Comparing facet temperature of standard and multi-section LDs at I_{las}=8 A for (a) L_{win}=500 μm with I_{win}=0 and 200 mA, and (b) L_{win}=1000 μm with I_{win}=0 and 400 mA.

Figure 6 compares T_{fac} of LDs having L_{win}=500 and 1000 μm with standard LD (L_{win}=0) at I_{las}=8 A with and without injecting I_{win}. Injecting I_{win} recovers output power and eliminates optical absorption in the window section resulting in further facet temperature reduction for both LDs. The output power and T_{fac} results confirm that pumping the window section at proper I_{win} values effectively recovers the power degradation with further cooling of the LD facet.

Finally, we executed high current test and failure analysis on LDs based on the above results. Figure 7(a) shows the L-I curves up to I_{las}=20 A (CW) and Figure 7(b) displays the top view of the laser cavity electroluminescence (EL) for the failed LDs. LD with L_{win}=0 μm reaches a maximum power of 13.1 W at I_{las}=14.5 A. Figure 7(b1) shows a COMD point and the dark line defects (DLDs) which extended from the facet into the active region. LD with L_{win}=500 μm at I_{win}=400 mA reaches a maximum power of 13.6 W at 15.5 A current, which is 0.5 W (1 A) higher than that of L_{win}=0 μm LD. From EL image of the LD in Figure 7(b2), it is apparent that the device is COMD-free and fails because of the catastrophic optical bulk damage

(COBD). The LD with L_{win}=1000 μm first tested with I_{win}=800 mA reaching a maximum power of 13.3 W at I_{las}=16 A where the maximum current is 1.5 A larger than that of L_{win}=0 μm LD. Afterward, the power drops to zero without showing COMD or COBD. LD tested many times under the same operation condition and showed no sign of power degradation. Then, I_{win} increased to 1000 mA and it was when the device failed Figure 7(b3) reaching a maximum power of 12.9 W at I_{las}=14 A. EL image clarifies that this device is also COMD-free where DLDs originate in the laser section.

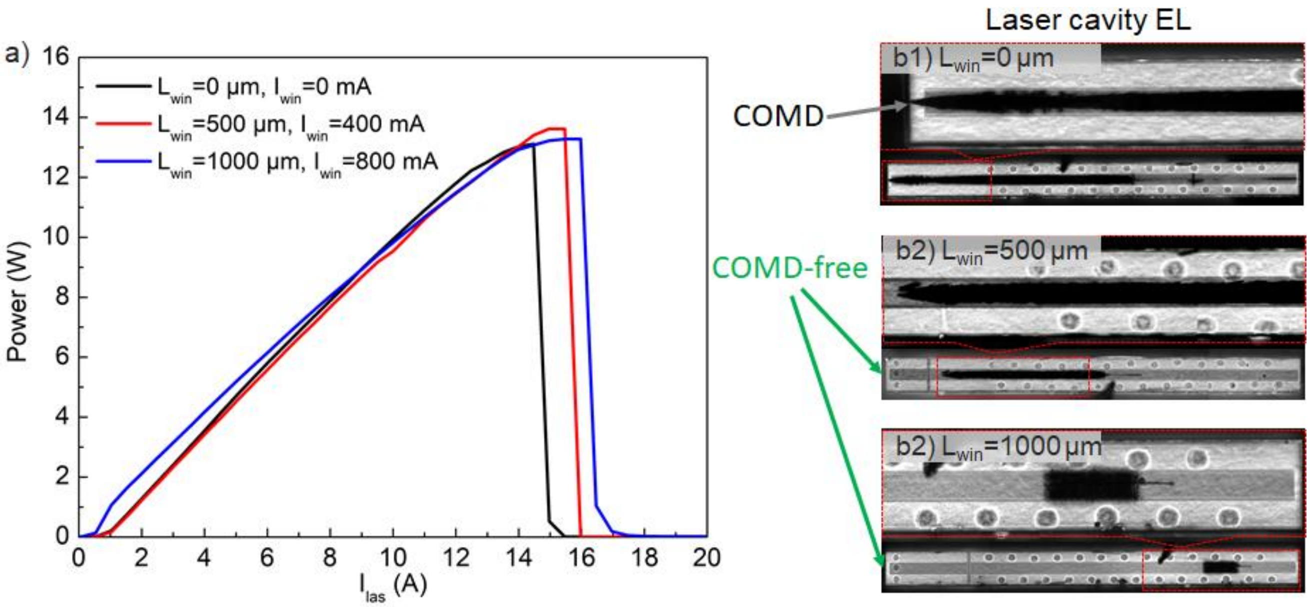

Figure 7. LDs failure test. (a) Output power versus current for LDs with L_{win}=0, 500, and 1000 μm under CW, 20°C operation. (b) EL image of the laser cavity.

Although multi-section LDs have higher current densities and T_{las} because of having smaller L_{las} than standard LD, similar output power levels are achievable under optimized conditions. Moreover, the higher current densities make multi-section LDs more vulnerable to COBD. Therefore, LDs can be designed with a fixed L_{las} length, while L_{win} is added as a cooling section, improving the reliability of LDs. Also, by implementing epi-down assembly, T_{las} could be reduced even further. Exploiting this combination COMD-free LDs can have further improvement in reliability.

4. CONCLUSION

This study addressed the dominant failure mode of conventional LD, catastrophic optical mirror damage (COMD). It offers a promising solution to such a long-standing vital issue with experimental results utilizing the multi-section LD technique. Detailed characterization of laser performance and facet temperatures of GaAs-based high-power multi-section LDs have been done. The optimum design and working conditions were obtained where LDs with 500 and 1000 μm window length operated COMD-free. The idea of multi-section LD presented here can also be applied to high-power laser arrays to improve reliability. Moreover, it would be beneficial to investigate the method of multi-section LD with epi-down configuration and long-term reliability studies.

Acknowledgement

The authors gratefully acknowledge the financial support in part from TUBITAK 118F057.

REFERENCES

[1] E. Zucker, D. Zou, L. Zavala, H. Yu, P. Yalamanchili, et al. “Advancements in laser diode chip and packaging technologies for application in kW-class fiber laser pumping,” Proc. SPIE 8965, 896507-1 (2014).

[2] V. Rossin, M. Peters, A Demir, J. J. Morehead, J. Guo, Y. Xiao, J. Cheng, A. Hsieh, R. Duesterberg, J. Skidmore, “High power, high brightness diode lasers for KW laser systems,” Proceedings of the 2015 High Power Diode Lasers and Systems Conference (HPD), 35-36 (2015).

[3] H. Wenzel, P. Crump, A. Pietrzak, X. Wang, G. Erbert, and G. Tränkle, “Theoretical and experimental investigations of the limits to the maximum output power of laser diodes,” New Journal of Physics, vol. 12, no. 8, p. 085007, Aug. 2010, doi: 10.1088/1367-2630/12/8/085007.

[4] A. Demir, et al. "Semiconductor laser power enhancement by control of gain and power profiles." IEEE Phot. Tech. Lett. 27.20 (2015): 2178-2181.

[5] A. Demir, et al. "29.5 W continuous wave output from 100 um wide laser diode." High-Power Diode Laser Technology and Applications XIII. Vol. 9348. International Society for Optics and Photonics, 2015.

[6] M. Ziegler et al., “Physical limits of semiconductor laser operation: A time-resolved analysis of catastrophic optical damage,” Appl. Phys. Lett., vol. 97, no. 2, p. 021110, Jul. 2010.

[7] M. Hempel, J. W. Tomm, M. Ziegler, T. Elsaesser, N. Michel, and M. Krakowski, “Catastrophic optical damage at front and rear facets of diode lasers,” Applied Physics Letters, vol. 97, no. 23, p. 231101, Dec. 2010, doi: 10.1063/1.3524235.

[8] J. Michaud et al., “Precise facet temperature distribution of high- power laser diodes: Unpumped window effect,” IEEE Photonics Technology Letters, vol. 27, no. 9, pp. 1002–1005, May 2015, doi: 10.1109/LPT.2015.2405090.

[9] R. M. Lammert, J. E. Ungar, M. L. Osowski, H. Qi, M. A. Newkirk, and N. Bar Chaim, “980-nm master oscillator power amplifiers with nonabsorbing mirrors,” IEEE Photonics Technology Letters, vol. 11, no. 9, pp. 1099–1101, Sep. 1999, doi: 10.1109/68.784169.

[10] L. W. Tu, E. F. Schubert, M. Hong, and G. J. Zydzik, “In-vacuum cleaving and coating of semiconductor laser facets using thin silicon and a dielectric,” Journal of Applied Physics, vol. 80, no. 11, p. 6448, Jun. 1998, doi: 10.1063/1.363664.

[11] P. Ressel et al., “Novel passivation process for the mirror facets of Al-free active-region high-power semiconductor diode lasers,” IEEE Photonics Technology Letters, vol. 17, no. 5, pp. 962–964, May 2005, doi: 10.1109/LPT.2005.846750.

[12] Epperlein P W 2013 Semiconductor Laser Engineering,Reliability and Diagnostics: A Practical Approach to High Power and Single Mode Devices (UK: Wiley) ch 4.

[13] H. Naito, T. Nagakura, K. Torii, M. Takauji, H. Aoshima, et al., Long-Term Reliability of 915-nm Broad-Area Laser Diodes Under 20-W CW Operation, IEEE Photonics Technology Letters 27(15) (2015) 1660-1662.

[14] S. Arslan, A. Demir, S. Şahin, and A. Aydinli, “Conservation of quantum efficiency in quantum well intermixing by stress engineering with dielectric bilayers,” Semiconductor Science and Technology, vol. 33, no. 2, p. 025001, Jan. 2018, doi: 10.1088/1361-6641/AAA04D.

[15] P. G. Piva et al., “Reduction of InGaAs/GaAs laser facet temperatures by band gap shifted extended cavities,” Appl. Phys. Lett., vol. 70, no. 13, pp. 1662–1664, Mar. 1997.

[16] F. Rinner et al., “Facet temperature reduction by a current blocking layer at the front facets of high-power InGaAs/AlGaAs lasers,” J. Appl. Phys., vol. 93, no. 3, pp. 1848–1850, 2003.

[17] S. Arslan, S. Gundogdu, A. Demir, and A. Aydinli, “Facet cooling in high-power InGaAs/AlGaAs lasers,” IEEE Photonics Technology Letters, vol. 31, no. 1, pp. 94–97, Jan. 2019, doi: 10.1109/LPT.2018.2884465.

[18] A. Demir, S. Arslan, S. Gündogdu, and A. Aydinli, “Reduced facet temperature in semiconductor lasers using electrically pumped windows,” Mar. 2019, p. 24. doi: 10.1117/12.2509896.

[19] Y. Liu, G. Yang, Z. Wang, T. Li, S. Tang, Y. Zhao, Y. Lan, and A. Demir, “High-power operation and lateral divergence angle reduction of broad-area laser diodes at 976 nm,” Opt. Laser Technol. 141, 107145 (2021).

[20] Y. Lan, G. Yang, Y. Liu, Y. Zhao, Z. Wang, T. Li, and A. Demir, “808 nm broad-area laser diodes designed for high efficiency at high-temperature operation,” Semicond. Sci. Technol. 36, 105012 (2021).

[21] P.-W. Epperlein, “Micro-temperature measurements on semiconductor laser mirrors by reflectance modulation: A

newly developed technique for laser characterization," Japanese J. Appl. Phys., vol. 32, no. 12A, pp. 5514–5522, Dec. 1993.
[22] M. Farzaneh et al., "CCD-based thermoreflectance microscopy: Principles and applications," Journal of Physics D: Applied Physics, vol. 42, no. 14, 2009, doi: 10.1088/0022-3727/42/14/143001.
[23] D. Pierścińska, "Thermoreflectance spectroscopy—Analysis of thermal processes in semiconductor lasers," Journal of Physics D: Applied Physics, vol. 51, no. 1, p. 013001, Nov. 2017, doi: 10.1088/1361-6463/AA9812.
[24] A. K. Jha et al., "Thermoreflectance-Based Measurement of Facet Optical Absorption in High Power Diode Lasers,"IEEE Photonics Technology Letters, vol. 31, no. 24, pp. 1909–1912, Dec. 2019, doi: 10.1109/LPT.2019.2949281.